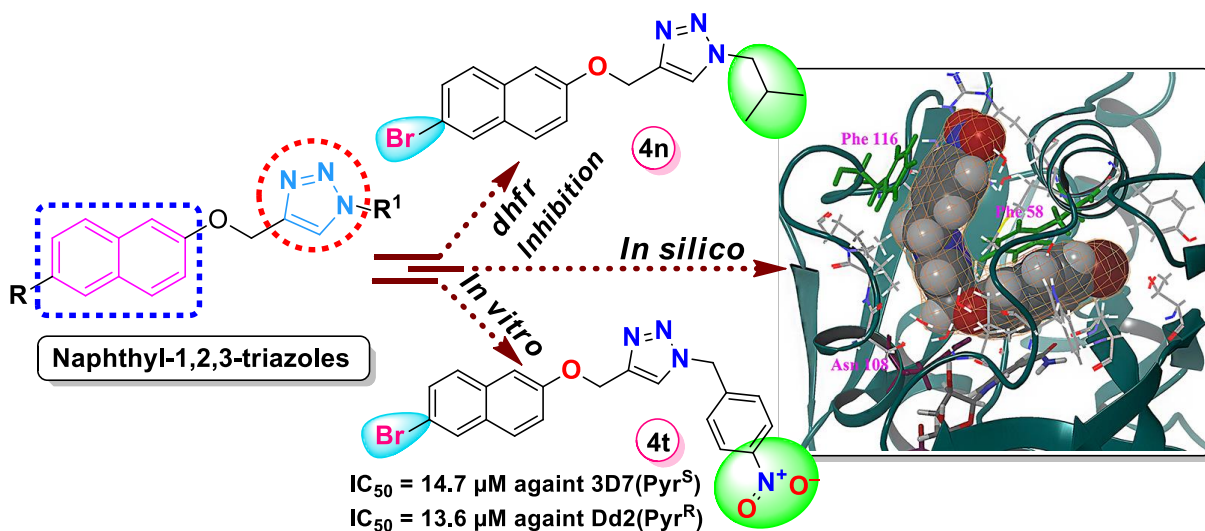


EXECUTIVE SUMMARY

University Grants Commission
Major Research Project
42-233/2013(SR)

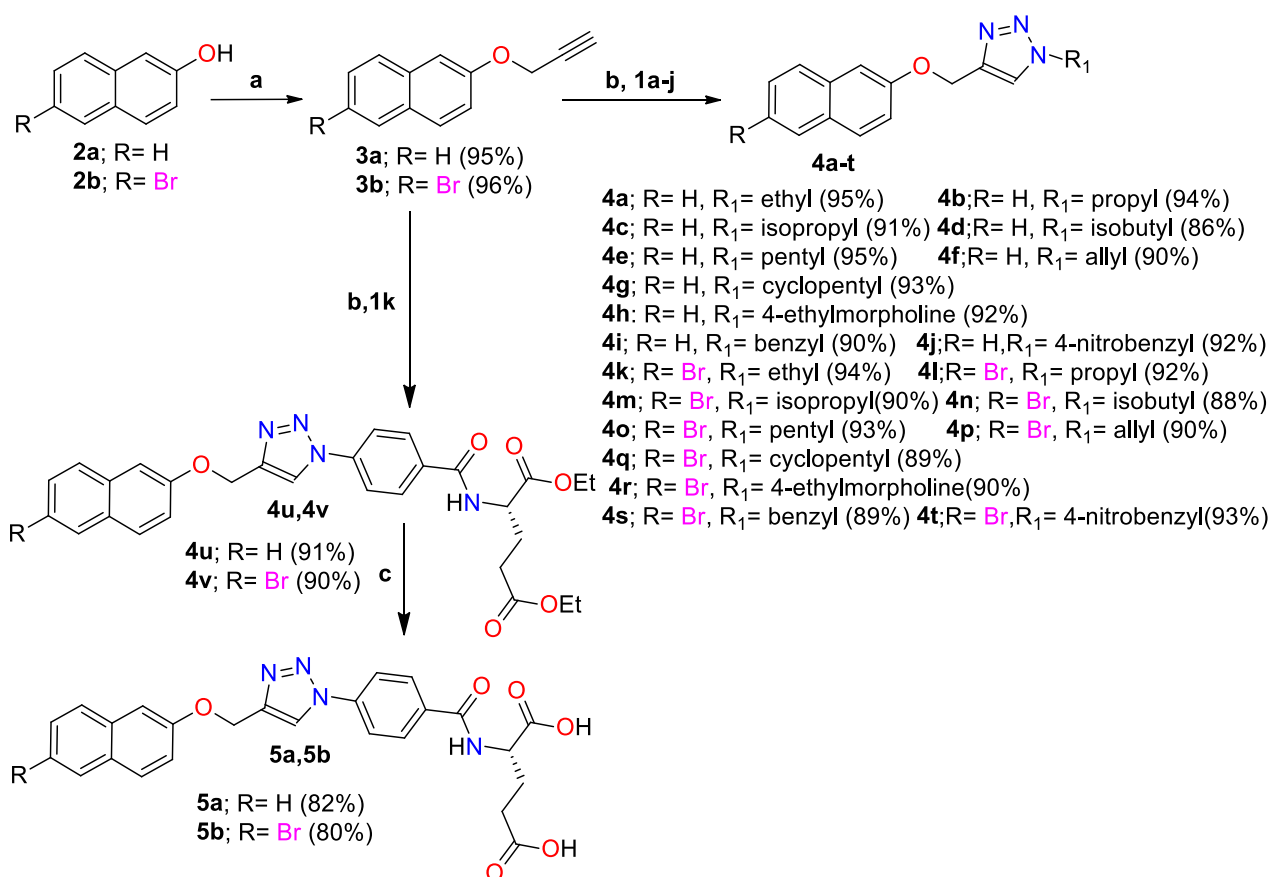
Combining Multiple Receptor Conformation Docking and 3D QSAR protocols for identification and design of novel Cycloguanil derivatives as *Plasmodium falciparum* DHFR inhibitors”

Novel series of naphthyl bearing 1,2,3-triazoles (**4a-t**) were synthesized and evaluated for their in vitro antiplasmodial activity against pyrimethamine (Pyr)-sensitive and resistant strains of *Plasmodium falciparum*. The synthesized compounds were assessed for their cytotoxicity employing human embryonic kidney cell line (HEK-293), and none of them was found to be toxic. Among them **4j**, **4k**, **4l**, **4m**, **4n**, **4t** exhibited significant antiplasmodial activity in both strains, of which compounds **4m**, **4n** and **4t** (~3.0 fold) displayed superior activity to Pyr against resistant strain. Pyr and selected compounds (**4n**, **4p** and **4t**) that repressed parasite development also inhibited PfDHFR activity of the soluble parasite extract, suggesting that anti-parasitic activity of these compounds is a result of inhibition of the parasite DHFR. In silico studies suggest that activity of these compounds might be enhanced due to π - π stacking.



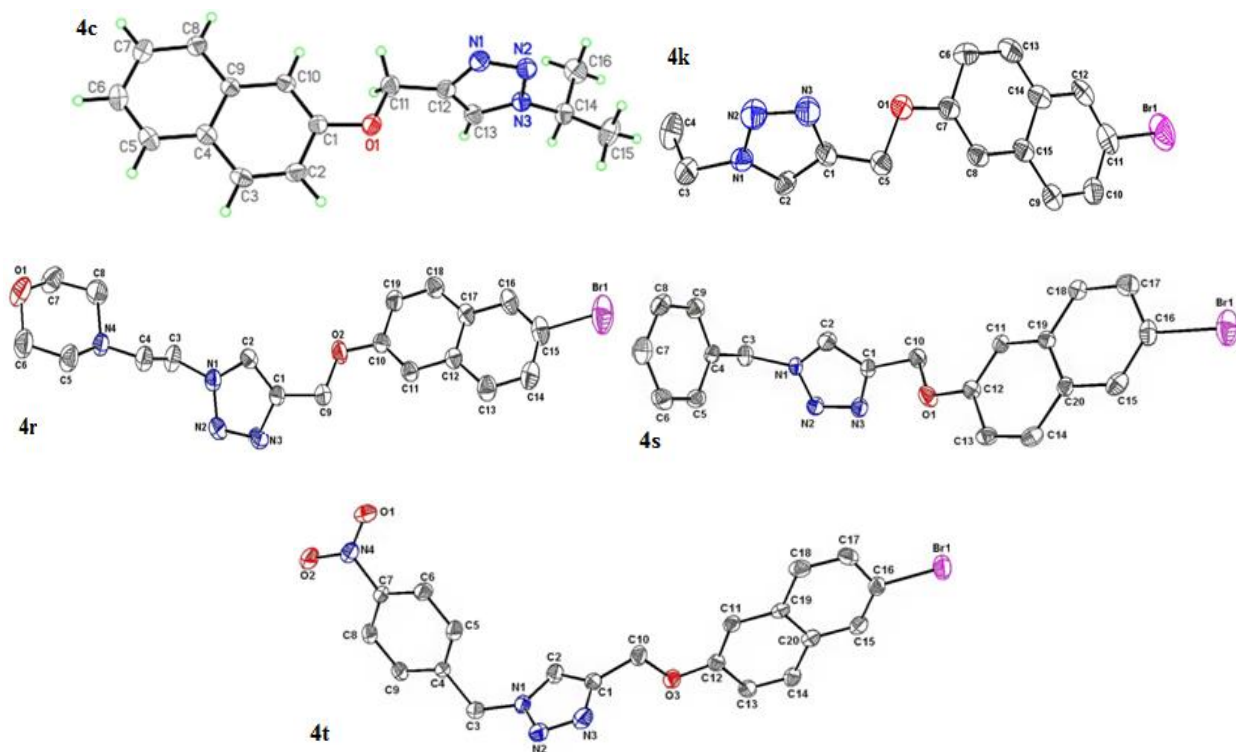
Synthesis of novel naphthyl 1,2,3-triazole derivatives **4a-v**, **5a** and **5b**.

Reagents and conditions; a) K_2CO_3 (1.1 equiv), propargyl bromide (1.1 equiv), in DMF refluxed for 3 h; b) azide **1a-1j,1k** (0.75 mmol), alkynes **3a, 3b** (1.05 equiv), $CuSO_4 \cdot 5H_2O$ (5 mol %), and Na ascorbate (15 mol %), in *t*-BuOH:H₂O (2:1) (10 mL) at room temp. for 12 h; c) THF:H₂O (15 mL), 1N NaOH(7.5 mL) at room temperature for 4 h. Reported yields are for the isolated products.



All the synthesized compounds are characterized by spectroscopic (¹HNMR, ¹³CNMR, LC-MS and HRMS) data and were found to be in good compliance with their depicted structures. Additionally, the structure of compounds **4c**, **4k**, **4r**, **4s** and **4t** were further confirmed by single crystal X-ray diffraction method. Fig. 2 shows a perspective view of these compounds together with their atomic labeling. Crystallographic data and structure refinement for these compounds is

provided in supporting information. Crystallographic data has been deposited for compounds **4c**, **4k**, **4r**, **4s** and **4t** with the Cambridge Crystallographic Data Centre [CCDC 1037001/2/3/4/5 respectively].



ORTEP drawings (30% probability level) for **4c**, **4k**, **4r**, **4s** and **4t**.

The newly synthesized compounds were evaluated for their antiplasmodial activity against Pyr-sensitive (3D7) and resistant (Dd2) *P. falciparum* strains. Selected 3D7 high active compounds (**4j**, **4k**, **4l**, **4m**, **4n** and **4t**) were assessed for antiplasmodial activity on Dd2 strain. Notably, all these compounds inhibited the growth of Dd2 with similar concentrations to that of wild type strain. The IC_{50} values of these compounds are summarized in Table 1, and their distribution was configured graphically as shown in Fig. 3. The compounds **4m** (IC_{50} of 24.0 μ M), **4n** (IC_{50} of 31.03 μ M) and **4t** (IC_{50} of 13.6 μ M) against Pyr resistant Dd2 strain showed improved antiplasmodial activity than the control drug Pyr (IC_{50} of 33.95 μ M).

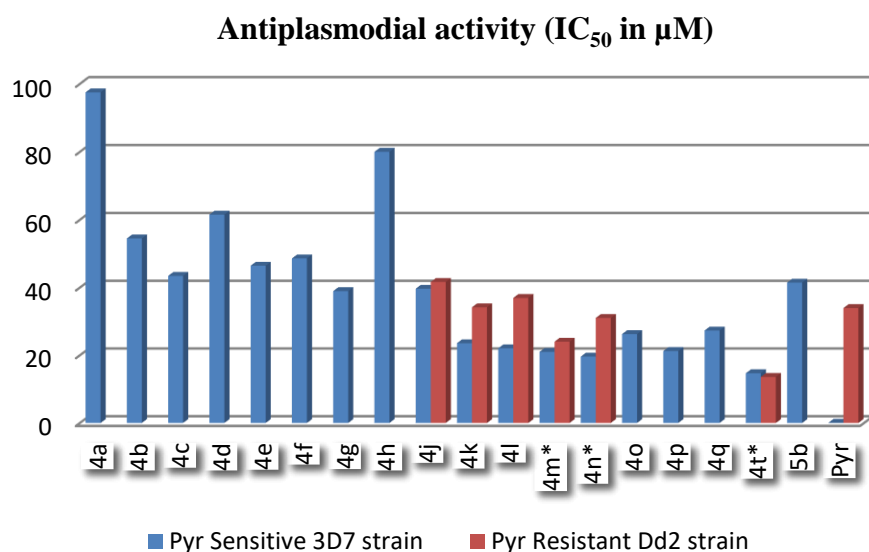
In vitro antiplasmodial activity^a and Cytotoxicity^b of the synthesized compounds.

Compound ID	P. falciparum 3D7	P. falciparum Dd2	IC ₅₀ +SEM (μM)
	IC ₅₀ in μM	IC ₅₀ in μM	HEK-293
4a	97.5	–	NC
4b	54.5	–	NC
4c	43.45	–	NC
4d	61.5	–	NC
4e	46.45	–	NC
4f	48.6	–	NC
4g	38.95	–	NC
4h	80	–	NC
4i	NA	–	–
4j	39.65	41.65	NC
4k	23.55	34.16	NC
4l	22.05	36.93	NC
4m*	21.0	24.0	NC
4n*	19.6	31.03	NC
4o	26.25	–	NC
4p	21.25	–	NC
4q	27.3	–	NC
4r	NA	–	–
4s	NA	–	–
4t*	14.7	13.6	NC
4u	NA	–	–
4v	NA	–	–
5a	NA	–	–
5b	41.45	–	NC

Pyr	0.047	33.95	–
Doxorubicin	–	–	3.13 ± 0.01

^a Pyr was used as a control drug. The IC₅₀ values are average with a standard deviation from two independent experiments, each done in duplicates. NA: Not Active (Did not inhibit, even at the highest concentration used), – : not determined. *More potent than Pyr against resistant strain.

^b Cell line was treated with different concentrations 1μM to 100μM of compounds for 48 h. Cell viability was measured employing MTT assay. IC₅₀ values are indicated as the mean +/- SD of three independent experiments. NC: Non Cytotoxic.



Graphical representation of antiplasmodial activity.

- New series of naphthyl bearing 1,2,3-triazoles were synthesized with good yields.
- Novel azide of (*S*)-diethyl-2-(4-azidobenzamido)pentanedioate was synthesized.
- Structures of **4c**, **4k**, **4r**, **4s** and **4t** have been studied by single crystal XRD.
- **4m**, **4n** and **4t** showed potent antiplasmodial activity compared to Pyrimethamine.
- Induced fit docking studies were performed for active compounds.

UNIVERSITY GRANTS COMMISSION
BAHADUR SHAH ZAFAR MARG
NEW DELHI – 110 002

PROFORMA FOR SUBMISSION OF INFORMATION AT THE TIME OF SENDING THE
FINAL REPORT OF THE WORK DONE ON THE PROJECT

1. Title of the Project “Combining Multiple Receptor Conformation Docking and 3D QSAR protocols for identification and design of novel Cycloguanil derivatives as *Plasmodium falciparum* DHFR inhibitors”
2. NAME AND ADDRESS OF THE PRINCIPAL INVESTIGATOR **Dr.M.Vijjulatha**,
Department of Chemistry, University College of Science, Osmania University,
Hyderabad 500 007, Telangana State
3. NAME AND ADDRESS OF THE INSTITUTION Osmania University Hyderabad 500
007, Telangana State
4. UGC APPROVAL LETTER NO. AND DATE **42-233/2013(SR), 12th March 2013**
5. DATE OF IMPLEMENTATION **1st April, 2013**
6. TENURE OF THE PROJECT **1st April, 2013 to 31st March, 2017**
7. TOTAL GRANT ALLOCATED 15,56,200/- (Fifteen lakhs fifty six thousand two hundred)
8. TOTAL GRANT RECEIVED 9,18,800/- (Nine lakhs eighteen thousand eight hundred)
9. FINAL EXPENDITURE 15,30,667/- (Fifteen lakhs thirty thousand six hundred and sixty seven)
10. TITLE OF THE PROJECT “Combining Multiple Receptor Conformation Docking and 3D QSAR protocols for identification and design of novel Cycloguanil derivatives as *Plasmodium falciparum* DHFR inhibitors”
11. OBJECTIVES OF THE PROJECT
 - ❖ Identify diverse protein targets and construct the pharmacophore model based on several X-ray crystal structures of protein-ligand complexes.
 - ❖ Three dimensional structure activity relationship (3D QSAR) analyses on the known inhibitors will be done. Based on this information new molecules will be designed and check for their predicted activity.

- ❖ Our computationally designed molecules will be checked for their characteristic requirements like low Molecular weight, cyclic structure in the scaffolds, since they provide molecular rigidity, allowing less entropy to be lost upon binding to the receptors and also providing better bioavailability. In addition to the above characteristic medicinal chemist's favorite suite of descriptors like rotatable bonds, polar surface area and Lipinski's drug like characteristics will be applied to calculate the ADME properties.
- ❖ These molecules will be docked into the diverse receptors to check for their binding affinities and their dock scores.
- ❖ The molecules having better binding interactions and high dock score will be taken for synthetic studies. After synthesizing these molecules their activity studies will be conducted either spectrophotometrically or by biological assay.

12. WHETHER OBJECTIVES WERE ACHIEVED (Please give details) **Yes**

Diverse targets Identified:

1. *Plasmodium falciparum* Dihydrofolate reductase (Pf DHFR)
2. *Plasmodium falciparum* Enol-Acyl Carrier protein reductase (Pf-ENR)
3. *Plasmodium falciparum* N-Myristoyl Transferase (Pf NMT)

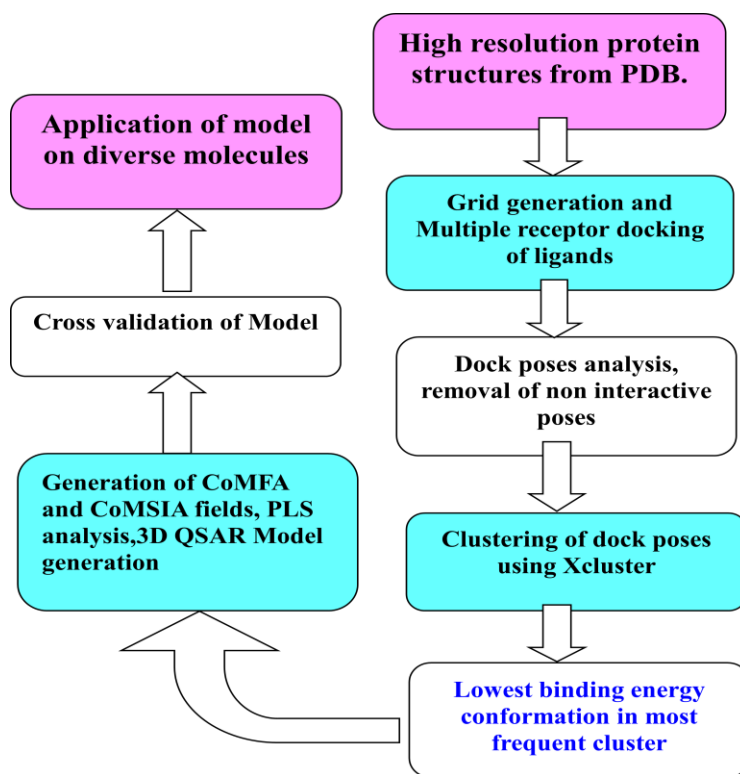
Computational studies on Pf Dihydrofolate reductase (Pf -DHFR):

Multiple Receptor Conformation docking and 3D QSAR studies:

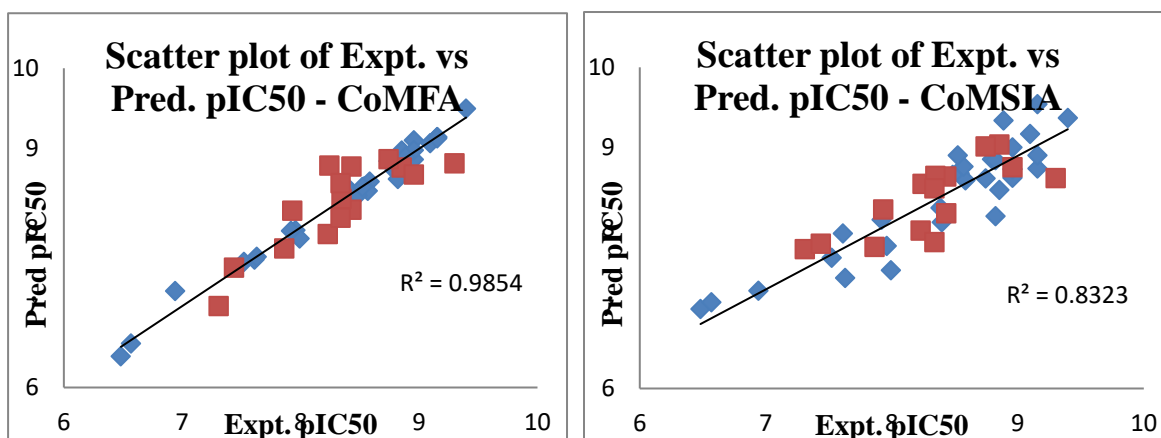
Five high resolution X-ray crystal structure of Pf DHFR in complex with inhibitors (pdb id: 1J3I, 3DGA, 3QGT, 3UM8 and 4DPD) were downloaded from the protein data bank. GLIDE 5.6 was used for molecular docking. Proteins were prepared using protein preparation module applying the default parameters, grids were generated around the active site of Pf DHFR with receptor van

der Waals scaling for the non-polar atoms as 0.9. Known Pf DHFR inhibitors with diverse structures and varied range of inhibition constants (K_i) were selected from literature, these were built using maestro build panel. Low energy conformers were obtained from LigPrep application in Schrödinger 2010 suite using the MMFF94s force field. These ligands were selected and docked into the grid generated from five protein structures using standard precision docking mode. The crystal structure ligands were also docked and its atomic root mean square deviation (RMSD) was calculated to validate docking process. The best dock pose (low binding energy conformer according to the glide dock score) of each ligand from five docking runs performed on five receptors grids were analyzed for their specific hydrogen bond interaction (Lys 165) with the receptor.

Methodology applied:



Docked poses were selected as is for further 3D-QSAR analysis using CoMFA and CoMSIA methodology. Gasteiger-Hückel charges were applied to the molecules. CoMFA and CoMSIA field were calculated using SYBYL-X 1.2. The molecules were divided into training and test set, a PLS analyses was performed and QSAR models were generated using 30 molecules in training set by applying leave one out cross validation method. Developed models showed good statistical reliability which is evident from r^2_{ncv} and r^2_{loo} values. The predictive ability of these models was determined using a test set of 11 molecules that gave predictive correlation (r^2_{pred}) of 0.719 and 0.59 for CoMFA and CoMSIA respectively. The information rendered from 3D QSAR model initiated us to optimize the lead and design new potential inhibitors.



Statistical Results of CoMFA and CoMSIA:

Statistical Parameters	CoMFA Model	CoMSIA Model
q ²	0.672	0.621
Molecules in training set	30	30
Molecules in test set	15	15
ONC	6	3

R2	0.985	0.832
SEE	0.104	0.331
F	257.843	43.027
R2pred	0.719	0.593
Fraction of Field Contributions:		
Steric	0.764	0.190
Electrostatic	0.236	0.337
Hydrophobic	-----	0.361
Donor	-----	0
Acceptor	-----	0.113

Pharmacophore Based Designing:

Dihydrofolate reductase (DHFR) enzyme is a major target for developing inhibitor for *Plasmodium falciparum* (Pf), a causative agent of malaria in humans. In order to study the key pharmacophore requirements for designing of new molecules three dimensional quantitative structure activity relationship (3D-QSAR) methodologies were applied. In order to obtain a better understanding of mechanism of action and structure activity relationship of Pf DHFR inhibitors, a Pharmacophore alignment and scoring engine (PHASE) analysis was performed and QSAR models were generated for a set of 59 reported 2-Methyl-6-Ureido-4-Quinolinamides. Five point pharmacophores with two hydrogen bond acceptor(A), one hydrogen bond donor(D) and two aromatic ring(R) as pharmacophore features were developed. AADRR yielded statistically significant 3D-QSAR model with 0.9002 as r^2 and 0.6275 as q^2 value. Results obtained from these studies can be used for rational design of potent inhibitors against Pf DHFR enzyme

Methodology:

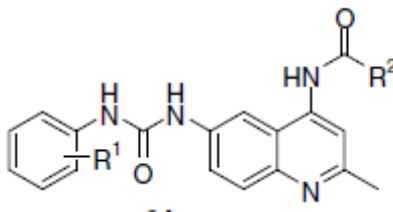
1. Pharmacophore Modeling:

Development of ligand based pharmacophore hypothesis for 2-methyl-6-ureido-4-quinolinamides analogues as potent inhibitors of *Plasmodium falciparum* DHFR was performed by using Schrodinger PHASE Module. PHASE module works as a following five steps process as:

1. Selection of training set
2. Generating conformers
3. Find hypothesis for actives
4. Score hypothesis.
5. Built QSAR model

This 3D-pharmacophore mapping approach involves the generation of a common pharmacophore hypothesis built on the principle of identification and alignment of pharmacophoric features of the chemical structures. QSAR models are then developed for the pharmacophore hypothesis using the training set structures that match the pharmacophore on three or more sites, using Partial Least Square (PLS) statistical analysis. The volume occluded maps, generated for the pharmacophore hypothesis help in explaining the observed variation in activity by the variation in the structural features.

Table 1: Molecule structure and their biological activities



Compound	R (13-17)/R ² (24-26)	R ¹	MIC (μg/mL)
13a	Ph	4-Cl	>50
13b	Ph	4-F	10
13c	Ph	4-Br	10
13d	Ph	3-Cl	50
13e	Ph	3-F	10
13f	Ph	3-CN	10
13g	Ph	3-CF ₃	10
13h	Ph	4-COMe	50
13i	Ph	3-COMe	10
13j	Ph	3-Cl-4-Me	2
13k	Ph	3-Cl-2-Me	50
13l	Ph	3,4-Cl ₂	1
13m	Ph	3,5-Cl ₂	2
13n	Ph	3-Cl-4-F	10
13o	Ph	4-Cl-3-CF ₃	1
14a	2-Cl-C ₆ H ₄	4-Cl	2
14b	2-Cl-C ₆ H ₄	4-F	50
14c	2-Cl-C ₆ H ₄	4-Br	2
14d	2-Cl-C ₆ H ₄	3-Cl	0.5
14e	2-Cl-C ₆ H ₄	3-F	2
14f	2-Cl-C ₆ H ₄	3-CN	1
14g	2-Cl-C ₆ H ₄	3-CF ₃	2
14h	2-Cl-C ₆ H ₄	4-COMe	2
14i	2-Cl-C ₆ H ₄	3-COMe	2
14j	2-Cl-C ₆ H ₄	3-Cl-4-Me	1
14k	2-Cl-C ₆ H ₄	3-Cl-2-Me	10
14l	2-Cl-C ₆ H ₄	3,4-Cl ₂	1
14m	2-Cl-C ₆ H ₄	3,5-Cl ₂	2
14n	2-Cl-C ₆ H ₄	3-Cl-4-F	10
14o	2-Cl-C ₆ H ₄	4-Cl-3-CF ₃	—
15a	3-Cl-C ₆ H ₄	4-Cl	1
15b	3-Cl-C ₆ H ₄	4-F	10
15c	3-Cl-C ₆ H ₄	4-Br	2
15d	3-Cl-C ₆ H ₄	3-Cl	50
15e	3-Cl-C ₆ H ₄	3-F	>50
15f	3-Cl-C ₆ H ₄	3-CN	1
15g	3-Cl-C ₆ H ₄	3-CF ₃	2
15i	3-Cl-C ₆ H ₄	3-COMe	10
15j	3-Cl-C ₆ H ₄	3,5-Cl ₂	10
15k	3-Cl-C ₆ H ₄	3-Cl-4-Me	1
15l	3-Cl-C ₆ H ₄	3-Cl-2-Me	10
15m	3-Cl-C ₆ H ₄	3,4-Cl ₂	2
15n	3-Cl-C ₆ H ₄	3-Cl-4-F	0.5
15o	3-Cl-C ₆ H ₄	4-Cl-3-CF ₃	>10
16a	2-furyl	4-Cl	0.5
16c	2-furyl	4-Br	1
16f	2-furyl	3-CN	0.5
16h	2-furyl	4-COMe	10
16j	2-furyl	3-Cl-4-Me	0.5
16l	2-furyl	3,4-Cl ₂	Insoluble
16m	2-furyl	3,5-Cl ₂	2
16o	2-furyl	4-Cl-3-CF ₃	—
17a	Me	4-Cl	10
17h	Me	4-COMe	10
17j	Me	3,5-Cl ₂	50

Compound	R (13-17)/R ² (24-26)	R ¹	MIC (μg/mL)
17m	Me	3-Cl-4-Me	2
24a		4-Cl	0.5
24b		4-F	2
24c		4-Br	1
24d		3-Cl	0.25
24e		3-F	10
24f		3-CN	2
24g		3-CF ₃	0.25
24h		4-COMe	1
24i		3-COMe	0.5
24j		3-Cl-4-Me	0.25
24k		3-Cl-2-Me	>10
24l		3,4-Cl ₂	0.25
24m		3,5-Cl ₂	0.25
24o		4-Cl-3-CF ₃	0.5
25g		3-CF ₃	0.5
25j		3-Cl-4-Me	0.5
25l		3,4-Cl ₂	2
25m		3,5-Cl ₂	2
26a		4-Cl	0.5

Dataset for analysis

A dataset comprising of 59 derivatives was used in the present study which is summarized in Table 1. The *in vitro* biological activity data was reported as MIC (minimum inhibition concentration). The MIC values were converted to pMIC, total of 59 molecules were available with pMIC values, of which 42 molecules were randomly chosen for training set and 17 molecules were selected for test sets.

Computational details for 3D QSAR

In the 3D-QSAR approach, all molecular modeling and statistical analyses were performed using PHASE. Pharmacophore Alignment and Scoring Engine (PHASE) is a highly flexible system for common pharmacophore identification and assessment, 3D-QSAR model development and 3D database creation and searching. PHASE is a versatile product for pharmacophore perception, structural alignment, activity prediction, and 3D database creation and searching. Given a set of molecules with affinity for a particular target, PHASE utilizes fine-grained conformational sampling and a range of scoring techniques to identify common pharmacophore hypothesis, which convey characteristics of 3D chemical structures that are purported to be critical for binding. Each hypothesis is accompanied by a set of aligned conformations that suggest the relative manner in which the molecules are likely to bind to the receptor. Generated hypothesis with the aligned conformations may be combined with known activity data to create a 3D-QSAR model that identifies overall aspects of molecular structure that govern activity. PHASE 3D-QSAR model workflow consists of the following five steps.

Preparing ligands

The 3D conversion and minimization was performed using LigPrep with OPLS 2005 force field¹⁶ incorporated in PHASE. Developing a pharmacophore model requires all-atom 3D structures that are realistic representations of the experimental molecular structure. Most ligands are flexible so it is important to consider a range of thermally accessible conformational states in order to increase the chances of finding something close to the putative binding mode. For purpose of pharmacophore model development, conformers were generated using a rapid torsion angle search approach followed by minimization of each generated structure using OPLS2005 force field, with implicit distance dependent dielectric solvent model. A maximum of 1000 conformers were generated per structure using a preprocess minimization of 100 steps and postprocess minimization of 50 steps. Each minimized conformer was filtered through a relative energy window of 10 kCal/mol and RMSD of 1.00 Å.

Creating pharmacophore sites

Each ligand structure is represented by a set of points in 3D space, which coincide with various chemical features that may facilitate noncovalent binding between the ligand and its target receptor. PHASE provides a built-in set of six pharmacophore features, hydrogen bond acceptor (A), hydrogen bond donor (D), hydrophobic group (H), negatively ionizable (N), positively ionizable (P), and aromatic ring (R). The rules that are applied to map the positions of pharmacophore sites are known as feature definitions, and they are represented internally by a set of SMARTS patterns. Each pharmacophore feature is defined by a set of chemical structure patterns. All user-defined patterns are specified as SMARTS queries and assigned one of the three possible geometries, which define physical characteristic of the site.

Finding a common pharmacophore

Pharmacophores from all conformations of the ligand in the active site are examined and those pharmacophores that contain identical sets of features with very similar spatial arrangements are grouped together. If a given group is found to contain at least one pharmacophore from each ligand, then this group gives rise to a common pharmacophore. Any single pharmacophore in the group ultimately become a common pharmacophore hypothesis which gives an explanation how ligands bind to the receptor. Common pharmacophores are identified using a tree based partitioning technique that groups together similar pharmacophores according to their inter site distances, i.e., the distances between pairs of sites in the pharmacophore. Active and inactive thresholds of P_{IC50} 5.4 and 5.1, respectively, were applied to the training set for developing the common pharmacophore hypotheses. After applying default feature definitions to each ligand, common pharmacophore containing five sites were generated using a terminal box size of 1 Å, and with requirement that all actives should match.

Scoring Hypotheses

In the score hypotheses step, common pharmacophores are examined, and a scoring procedure is applied to identify the pharmacophore from each surviving n-dimensional box that yields the best alignment of the active set ligands. This pharmacophore provides a hypothesis to explain how the active molecules bind to the receptor. The scoring procedure provides a ranking of the different hypotheses, allowing making rational choices about which hypotheses are most appropriate for further investigation. Scoring with respect to actives was conducted using default

parameters for site, vector, and volume terms. Ligand activity, expressed as $-\log_{10}(\text{IC}_{50})$, was incorporated into the score with a weight of 1.0, rest with default values. Hypotheses that emerged from this process were subsequently scored with respect to in actives, using a weight of 1.0. The inactive molecules were scored to observe the alignment of these molecules with respect to the pharmacophore hypothesis to enable making a decision on the selection of the hypothesis. Larger is the difference between the scores of active and inactives better is the hypothesis at distinguishing the actives from inactives.

Building QSAR model

PHASE provides the means to build QSAR models using the activities of the ligands that match a given hypothesis. PHASE QSAR models are based on PLS regression, applied to a large set of binary valued variables. The independent variables in the QSAR model are derived from a regular grid of cubic volume elements that span the space occupied by the training set ligands. Each ligand is represented by a set of bit values (0 or 1) that indicate which volume elements are occupied by a van der Waals surface model of the ligand. To distinguish different atom types that occupy the same region of space, a given cube in the grid may be allocated as many as six bits, accounting for six different classes of atoms. The atoms classes are: D: hydrogen-bond donor, H: hydrophobic or nonpolar, N: negative ionic, P: positive ionic, W: electron-withdrawing (includes hydrogen-bond acceptors), X: miscellaneous (all other types).

PHASE QSAR models may be either atom-based or pharmacophore-based, the difference being whether all atoms are taken into account, or merely the pharmacophore sites that can be matched to the hypothesis. The choice of which type of model to create depends largely on whether or not the training set molecules are sufficiently rigid and congeneric. If the structures contain a relatively small number of rotatable bonds and some common structural framework, then an atom-based model may work quite well. Atom-based QSAR models were generated for AADRR41 hypothesis using 42 molecules training set and a grid spacing of 1.0\AA . QSAR models containing one to five PLS factors were generated. A model with fifth PLS factor was considered as the best statistical model. This model was validated by predicting activities of test set molecules.

Pharmacophore 3D-QSAR models were derived using a set of 59 reported 2-methyl-6-ureido-4-quinolinamides. Five point pharmacophores with two hydrogen bond acceptor(A), one hydrogen bond donor(D) and two aromatic ring(R) as pharmacophoric features were developed. Best pharmacophore developed is shown in figure 1. Figure 2 represents the QSAR model obtained for the set of molecules. Blue cubes represent favoured regions for substitution to enhance the activity. Red cubes represent disfavoured regions for substitution.

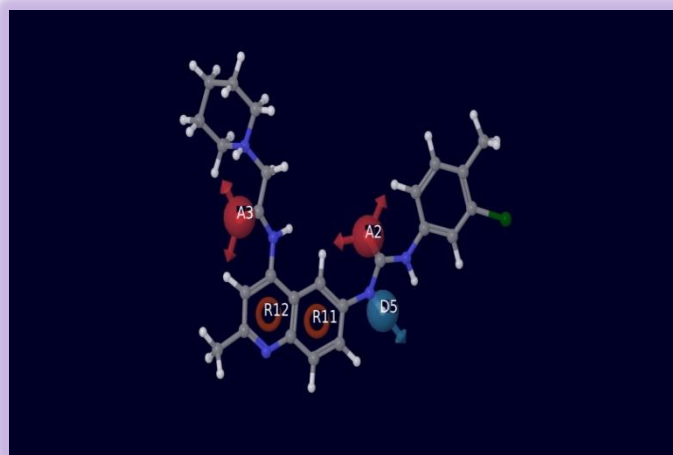


Figure: PHASE generated pharmacophore model AADRR of most active molecule illustrating hydrogen bond acceptor (A3, A2; pink), hydrogen bond donor (D5; cyan), aromatic ring (R11, R12; orange) features.

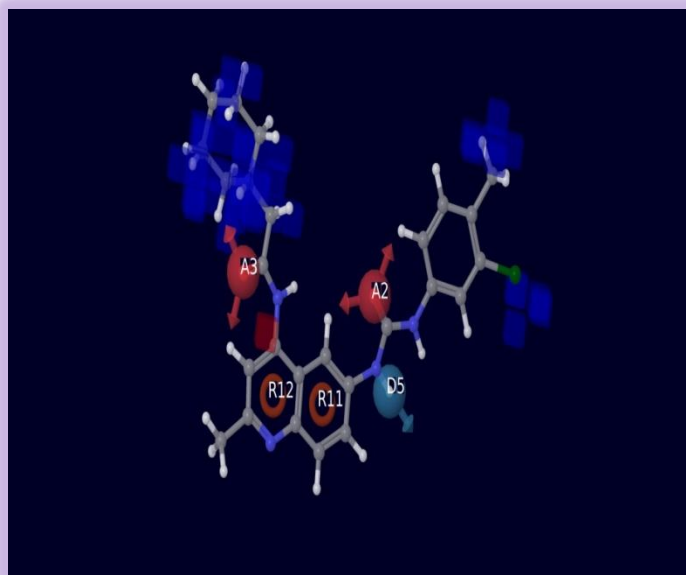


Figure: Pictorial representation of the cubes generated using the QSAR model of most active molecule . Blue cubes indicate favourable regions, while red cubes indicate unfavourable region for the activity

Developed QSAR model showed good statistical reliability, the generated model had a regression coefficient (R^2) value of 0.9002 and cross validated regression coefficient (Q^2) value of 0.627. This value indicates the ability of the model to predict the activity of test molecules, it is clear for the results that the model has 62.7% accuracy in predicting the activity of the molecules. Hence can be used to design and predict the activity of novel molecules. New molecules can be designed based on the pharmacophore model, designing of molecules should be done keeping in mind that the basic pharmacophoric feature should be kept intact, that is the acceptor, donor and aromatic ring system should be present in new molecules so that the required interaction with the receptor is maintained.

Based on developed pharmacophoric model, novel coumarin molecules were screened and designed.

Computational studies on *Plasmodium falciparum* Enol-Acyl Carrier protein reductase (Pf-ENR):

The elongation model of fatty acid biosynthesis pathway (FAS II) in *Plasmodium falciparum* has opened new opportunities for malaria drug development. Fatty acids play a vital role in cells as

metabolic precursors for biological membranes and energy storage. Many of FAS II enzymes are involved in malarial viability. The newly identified class of rhodanine inhibitors working against PfENR. Docking and 3D quantitative structure activity relationship (3D-QSAR) studies involve comparative molecular field analysis (CoMFA) and comparative molecular similarity indices analysis (CoMSIA) were performed on a series of rhodanine reported as inhibitors of pfENR. Ligands were built and docked into protein active site using GLIDE 5.6, the docked poses were analyzed, and the best docking poses were selected as is for further 3D-QSAR analysis using CoMFA and CoMSIA methodology. Gasteiger-Hückel charges were applied to the molecules. CoMFA and CoMSIA field were calculated using SYBYL-X 1.2 .The molecules were divided into training and test set, a PLS analyses was performed and QSAR models were generated using 42 molecules in training set by applying leave one out cross validation method. Developed models showed good statistical reliability which is evident from r^2_{ncv} and r^2_{loo} values. The predictive ability of these models was determined using a test set of 11 molecules that gave predictive correlation (r^2_{pred}) of 0.68 and 0.69 for CoMFA and CoMSIA respectively. The information rendered from 3D QASR model initiated us to optimize the lead and design new potential inhibitors

Enoyl-ACP reductase(FabI):

It is the last enzyme of fatty acid elongation cycle reduces the double bond of enoyl ACP using NADH as cofactor. This makes FabI an attractive target not only for antimalarials but also for various antibacterial

Methodology Applied:

The crystal structure of Enoyl-ACP reductase (FabI) (pdb id: 3LTI) was downloaded from the protein databank. GLIDE 5.6 was used for molecular docking. The protein was prepared using protein preparation module applying the default parameters, a grid was generated around the active site of the Pf-Enoyl-ACP reductase(FabI) with receptor van der Waals scaling for the nonpolar atoms as 0.9. A set of 53 known Pf-ENR inhibitors were selected from literature. These were built using maestro build panel and prepared by Lig prep application in Schrödinger 2010 suite. The molecular docking of the 53 molecules into the generated grid was performed by using the extra – precision (XP) docking mode. The crystal structure ligand was also docked and

its root mean square deviation (RMSD) was calculated to validate the docking process. The analysis of dock poses of all the molecules showed similar hydrogen bond interaction with the active site residue. The best dock pose for each molecule was chosen for CoMFA and CoMSIA analysis without further alignment that is super imposition of ligands based on the common substructure for a set of molecule was not done. The molecules were imported into SYBYLX1.2 molecular modeling program package, Gasteiger-Huckel charges were assigned. The standard Tripos force fields were employed for the CoMFA and CoMSIA analyses. A 3D cubic lattice of dimension 4Å in each direction with each lattice intersection of regularly spaced grid of 2.0Å was created. The steric and electrostatic parameters were calculated in case of the CoMFA fields while hydrophobic, acceptor and donor parameters in addition to steric and electrostatic were calculated in case of the CoMSIA fields at each lattice. The SP³ carbon was used as a probe atom to generate steric (Lennard Jones potential) field energies and a charge of +1 to generated electrostatic (Columbic potential) field energies. A distance dependented dielectric constant of 1.00 was used. The steric and electrostatic contributions were cut off at 30 k cal mol⁻¹.

A partial least squares (PLS) regression was used to generate a linear relationship that correlates changes in the computed fields with changes in the corresponding experimental values of biological activity (pKi) for the data set of ligands. The data set was divided into training set consisting of 42 molecules and test set of 11 molecules. Biological activity values of ligands were used as dependent variables in a PLS statistical analysis. The column filtering value (s) was set to 2.0 K cal mol⁻¹ to improve the signal-to-noise ratio by omitting those Lattice points whose energy variation were below this threshold. Cross-validation was performed by the leave-one-out (LOO) procedure to determine the optimum number of components (ONC) and the coefficient r^2_{100} . Optimum number of components obtained is then used to derive the final QSAR model using all of the training set compounds with non-cross validation and to obtain the conventional regression coefficient (r^2). To validate the CoMFA and CoMSIA derived models, the predictive ability for the test set compounds (expressed as r^2_{pred}) was determined by using the following equation.

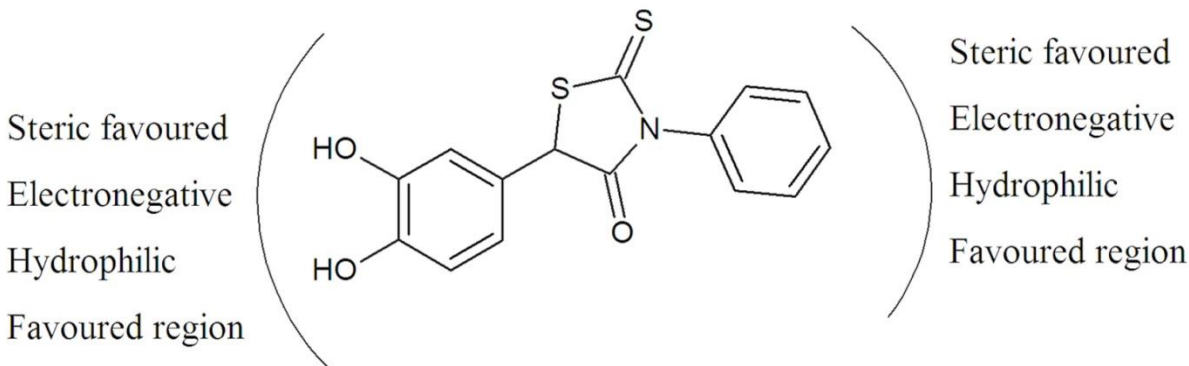
$$r^2_{pred} = (SD-PRESS)/SD$$

SD is the sum of the squared deviation between the biological activities of the test set molecules and the mean activity of the training set compounds. PRESS is the sum of the squared of the deviation between the observed and the predicted activities of the test set compounds. Since the statistical parameters were found to be the best for the model from the LOO method, it was employed for further prediction of the designed molecules. The designed molecules were also constructed, minimized and docked into the protein active site same as mentioned above.

Summary of PLS Analysis

Statistical Parameter	CoMFA	CoMSIA
No. of molecules in training set	42	42
No. of Molecules in test set	11	11
Q^2_{loo}	0.665	0.580
ONC	8	8
R^2	0.979	0.974
R^2_{pred}	0.680	0.690
SEE	0.095	0.106
F_{value}	194.018	153.801
Field Contributions in (%)		
Steric	45.3	9.7
Electrostatic	54.7	26.5
Hydrophobic	--	20.9
Hydrogen bond Donor	--	26.9
Hydrogen bond Acceptor	--	16.0

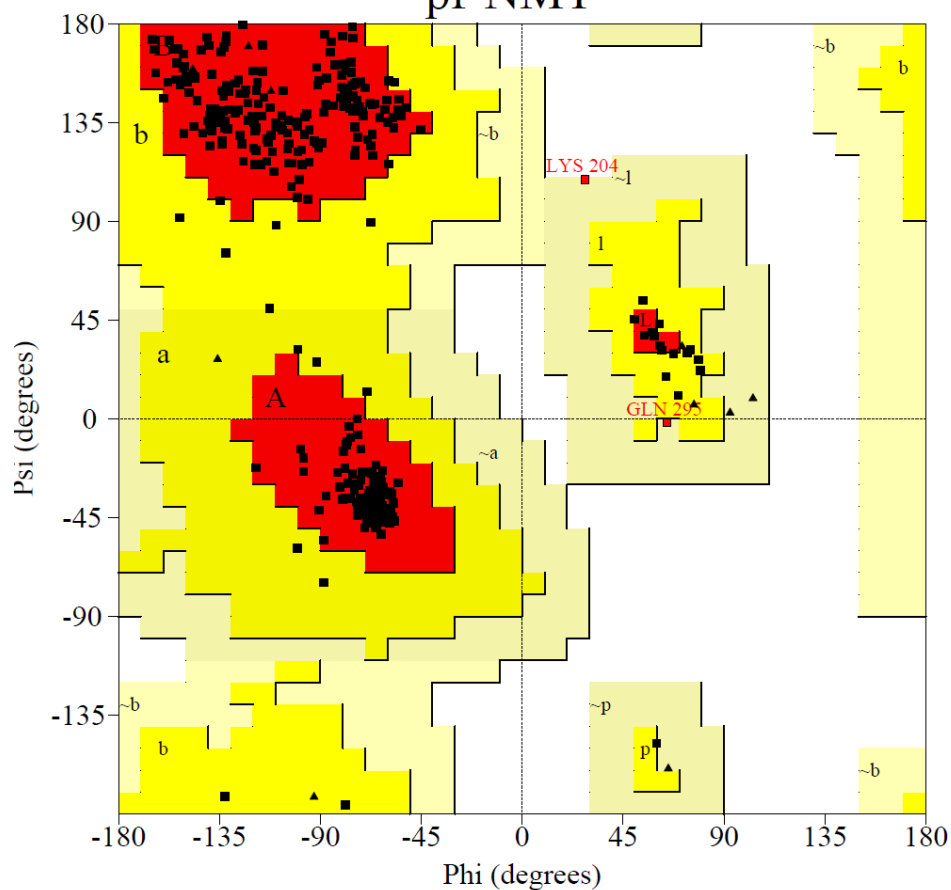
Structural requirement for Pf-ENR inhibitory activity deduced from 3D QSAR studies



Computational studies on *Plasmodium falciparum* N-Myristoyl Transferase (Pf-NMT):

An enzyme from the parasite, myristoylCoA:protein N-Myristoyl Transferase(NMT), has been identified as a potent target for antimalarial drugs. NMT which catalyses the co-translational transfer of myristic acid to the N-terminal of glycine of certain substrate proteins, has been shown to be essential for various pathogens. Since the X ray structure is not available for *Plasmodium falciparum*(Pf) NMT, an atomic resolution model of the protein was constructed using its homologous protein (the template) of *P.vivax* NMT with 81% sequence similarity using Homology Modelling. The present work demonstrates the design and study of potential inhibitors of *P. falciparum* NMT. In order to study the interactions between the potential inhibitors and the protein, docking studies were performed on modeled Pf NMT and crystallized PvNMT obtained from protein data bank. There was a good correlation between the dockscore and the biological activity inferring the correctness of modeled protein. To further understand the key pharmacophore requirements for designing new molecules 3D-QSAR studies were performed, that gave statistically reliable model which is instrumental for designing novel molecules with potent activity against Pf and Pv.

Ramachandran Plot pf-NMT



Plot statistics

Residues in most favoured regions [A,B,L]	334	93.0%
Residues in additional allowed regions [a,b,l,p]	23	6.4%
Residues in generously allowed regions [~a,~b,~l,~p]	2	0.6%
Residues in disallowed regions	0	0.0%

Number of non-glycine and non-proline residues	359	100.0%
Number of end-residues (excl. Gly and Pro)	4	
Number of glycine residues (shown as triangles)	12	
Number of proline residues	12	

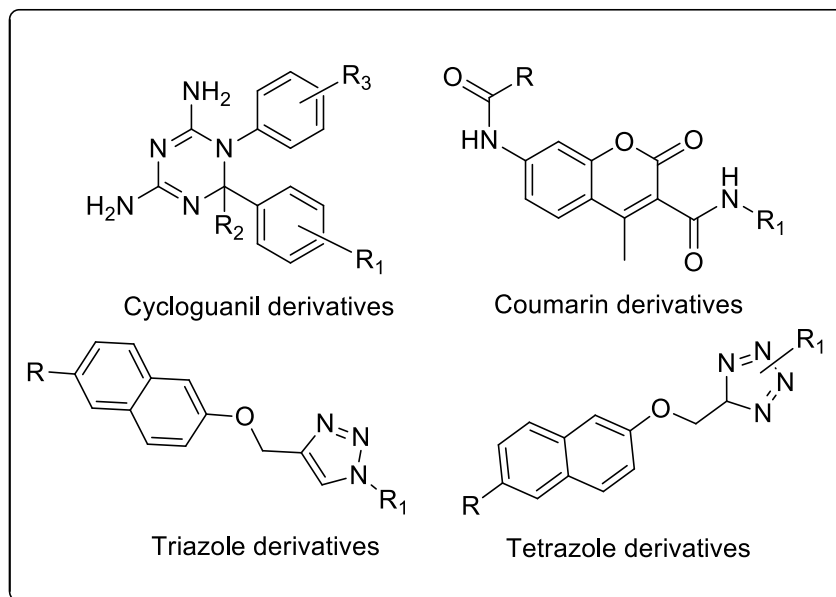
Total number of residues	387	

Based on an analysis of 118 structures of resolution of at least 2.0 Angstroms and R-factor no greater than 20%, a good quality model would be expected to have over 90% in the most favoured regions.

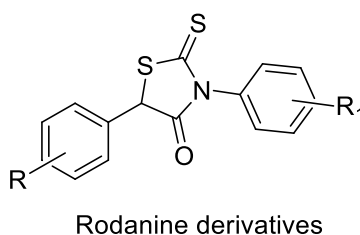
Structure validation – Ramachandran plot of modeled Pf-NMT

Designing of Novel Molecules:

Pf DHFR: Novel Cycloguanil derivatives, 1,4-disubstituted-1,2,3-triazole derivatives and 1,4-disubstituted-1,2,3,4-tetrazole derivatives were designed from Docking and QSAR studies. Based on pharmacophore based QSAR analysis Novel Coumarin derivatives were designed.



Pf-ENR: Novel rhodanine derivatives were designed as potent inhibitors of *Pf*ENR based on docking and CoMFA and CoMSIA studies.



Synthesis of Novel Molecules as Anti-malarial Agents.

All chemicals and reagents used in current study were analytical grade. Reactions were monitored by thin layer chromatography (TLC) on silica gel plates (60 F254), using UV light detection. Column chromatography was performed on silica gel (200-300 mesh) using solvent mixtures specified in the corresponding experiment. Spots were visualized by irradiation with ultraviolet light (254 nm). Melting points (mp) were taken in open capillaries and are

Solvent was removed under reduced pressure, and the azide was sufficiently pure to use without further purification.

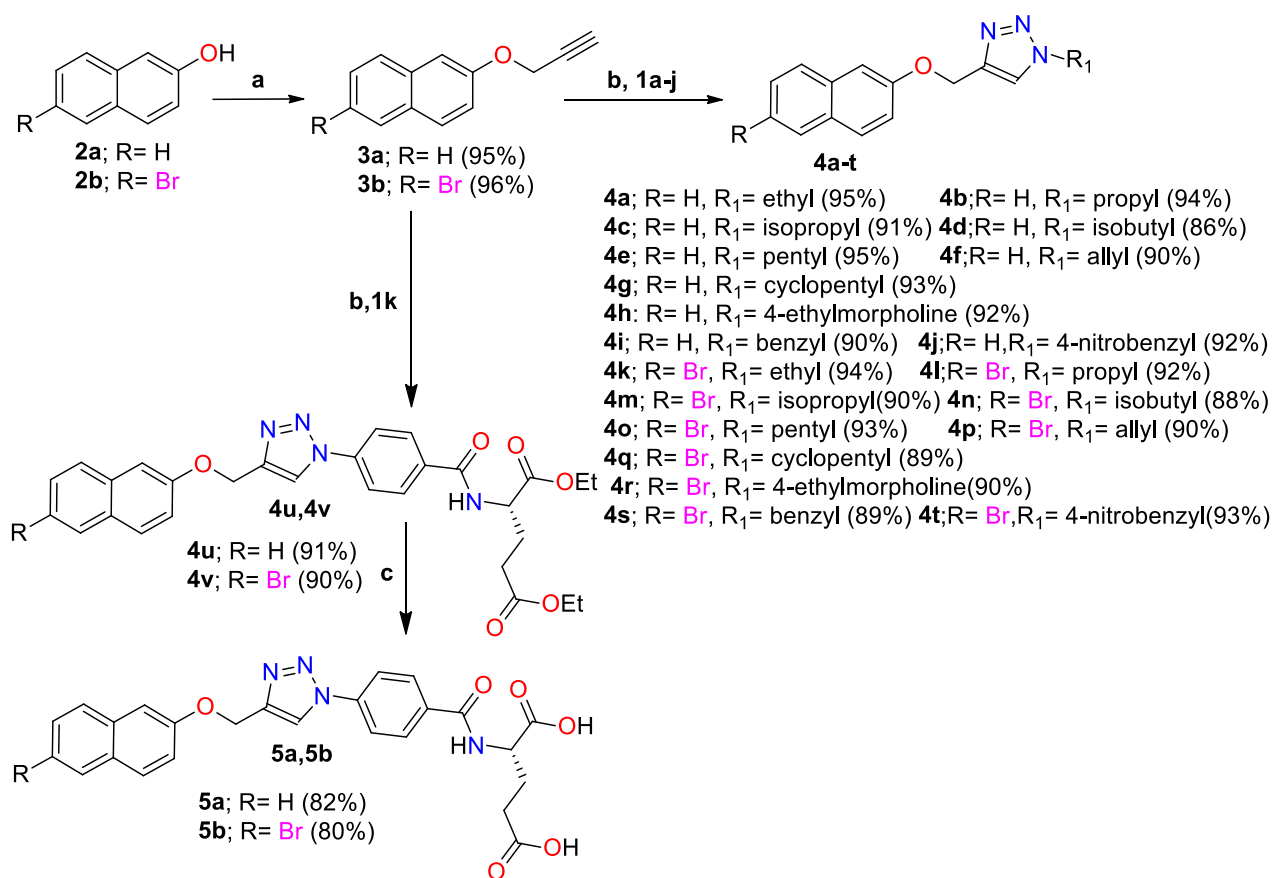


Scheme 2. Synthesis of novel (*S*)-diethyl-2-(4-azidobenzamido)pentanedioate (**1k**)

Typical Procedure for the Preparation of *S*-diethyl 2-(4-azidobenzamido)pentanedioate (**1k**):

To a mixture of L-diethyl 2-(4-aminobenzamido)pentanedioate (1.0 equiv) in acetonitrile, was added $t\text{-BuONO}$ (1.5 equiv) and TMSN_3 (1.2 equiv) at 0°C , the mixture was warmed to room temperature and stirred for 2h. The resulting mixture was poured into Hexane (5mL) and H_2O (5mL), and the organic layer was separated. The aqueous layer was extracted with Hexane (15mL) three times. The combined organic layer was concentrated in vacuo. The residue was purified by column chromatography on silica gel eluted with absolute dried hexane to afford a new L-diethyl 2-(4-azidobenzamido)pentanedioate in 92% isolated yield. The reaction proceeds smoothly and rapidly.

Light Yellow solid; $42\text{-}44^\circ\text{C}$; $^1\text{H NMR}$ (400 MHz, CDCl_3) δ 7.84 (2H, d, $J = 8.8$ Hz), 7.09 (2H, d, $J = 8.8$ Hz), 4.79-4.75 (1H, m), 4.27-4.23 (2H, m), 4.14-4.10 (2H, m), 2.54-2.41 (2H, m), 2.32-2.29 (1H, m), 2.20-2.12 (1H, m), 1.32 (3H, t, $J = 7.2$ Hz), 1.24 (3H, t, $J = 7.2$ Hz); $^{13}\text{C NMR}$ (100 MHz, CDCl_3) δ 173.5, 171.9, 166.1, 143.7, 130.1, 128.9, 119.0, 61.8, 60.9, 52.5, 30.5, 27.1, 14.2, 14.1 ppm.



Scheme 3. Synthesis of novel naphthyl 1,2,3-triazole derivatives **4a-v**, **5a** and **5b**.

General procedure for preparation of alkynes **3a** and **3b**:

To a suspension of appropriate 2-naphthol (0.1 mol) in DMF (10 mL) was added K₂CO₃ (0.11 mol) in DMF (10 mL). After the reaction was heated to 60°C for 30 min, a solution of 3-bromoprop-1-yne (0.11 mol) in DMF(5 mL) was added drop wise and the mixture was refluxed for 3h.(monitored by TLC; Hexane:EtOAc-9:1). The mixture was neutralized with dil. aqueous HCl and extracted with EtOAc(3x30 mL), dried over Na₂SO₄ and evaporated to dryness under reduced pressure to yield the crude product as light cream solid, purified by column chromatography (silica gel, Hexane:EtOAc-9:1 as developing solvent) obtained the desired product as white solid.

2-(prop-2-yn-1-yloxy)naphthalene (**3a**):

Light orange solid; mp: 48-50 °C ; ¹H NMR (400 MHz, CDCl₃) δ 7.79-7.75 (3H, m), 7.45 (1H, td, J = 5.6, 1.2 Hz), 7.36 (1H, td, J = 5.6, 1.2 Hz), 7.24 (1H, d, J = 2.4 Hz), 7.19 (1H, dd, J = 6.4, 2.4 Hz), 4.81 (2H, d, J = 2.4 Hz), 2.55 (1H, t, J = 2.4 Hz) ; ¹³C NMR (100 MHz, CDCl₃) δ 155.5, 134.3, 129.6, 129.3, 127.7, 126.9, 126.5, 124.0, 118.7, 107.5, 78.5, 75.7, 55.9 ppm.

2-bromo-6-(prop-2-yn-1-yloxy)naphthalene (3b):

Color less solid; mp: 70-72 °C ; ¹H NMR (400 MHz, CDCl₃) δ 7.93 (1H, d, J = 2.0 Hz), 7.64 (2H, m), 7.51 (1H, dd, J = 6.4, 2.0 Hz), 7.22-7.19 (2H, m), 4.80 (2H, d, J = 2.4 Hz), 2.56 (1H, t, J = 2.4 Hz) ; ¹³C NMR (100 MHz, CDCl₃) δ 155.7, 132.8, 130.4, 129.8, 129.7, 128.7, 128.6, 119.8, 117.5, 107.5, 78.2, 75.9, 55.9 ppm.

General procedure for the synthesis of compounds (4a-v):

In a round bottomed flask, Aryl/ Alkyl azide **1a-j,1k** (0.75 mmol) and naphthalen-2-ylprop-2-yn-1-yloether (**3a**) or 6-bromo naphthalen-2-ylprop-2-yn-1-yloether (**3b**) (1.05 equiv) were added to a mixture of copper(II) sulfate pentahydrate (9.4 mg, 0.05 equiv), and sodium ascorbate (23 mg, 0.15 equiv) dissolved in 2:1 of *t*-BuOH and H₂O (10 mL) at room temperature. The reaction mixture was stirred for 12 h at room temperature and was poured into ice cold water (20 mL). The aqueous layer was extracted with CH₂Cl₂ (10 mL) thrice. The combined organic layer was concentrated in vacuo. The residue was purified by short column chromatography on silica gel (70–230 mesh) eluted with hexane/ EtOAc (4/1) to afford the desired products **4a-v**.

General procedure for the synthesis of 5a and 5b:

A solution of corresponding ester (**4u/v**) (0.5 g) in H₂O:THF (1:1, 15 mL) was treated with 1N aqueous NaOH solution (7.5 mL) at room temperature for 4 h. THF was evaporated under

reduced pressure and 1N HCl solution was added drop wise to the residue. The white crystalline precipitate was collected by filtration, washed with water, and dried over CaCl₂ under vacuum to give **5a/b**.

Crystallographic studies:

Single-crystal structures of X-ray data were collected for **4c**, **4k**, **4r**, **3s**, and **3t** on a Bruker SMART APEX CCD X-ray diffractometer, using graphite-monochromated Mo-K α radiation ($\lambda = 0.71073 \text{ \AA}$). Data were reduced using SAINTPLUS and a multi-scan absorption correction using SADABS was performed. The structure was solved and refined against F^2 using SHELX-97. All ring hydrogen atoms were assigned on the basis of geometrical considerations and were allowed to ride upon the respective carbon atoms. All hydrogen atoms were assigned fixed U_{iso} values, equal to $1.2U_{\text{eq}}$ of the parent atom. Crystallographic data are presented in Table 2, and the molecular structures of **4c**, **4k**, **4r**, **4s**, and **4t** are illustrated in Figure 1 with 30% probability displacement ellipsoid.

Table 2: Crystallographic data and structure refinement for compound **4c, **4k**, **4r**, **4s**, and **4t****

Formula	C ₁₆ H ₁₇ N ₃ O	C ₁₅ H ₁₄ BrN ₃ O	C ₁₉ H ₂₁ BrN ₄	C ₂₀ H ₁₆ BrN ₃ O	C ₂₀ H ₁₅ BrN ₄
	(4c)	(4k)	O ₂ (4r)	(4s)	O ₃ (4t)
CCDC No.	1037001	1037002	1037003	1037004	1037005
Formula weight	267.33	332.20	417.31	394.27	439.27
Crystal system	Monoclinic	Monoclinic	Monoclinic	Orthorhombic	Orthorhombic
<i>a</i> (Å)	8.0073(19)	12.4217(17)	13.8024(16)	5.7143(8)	5.9881(13)
<i>b</i> (Å)	21.533(5)	5.4679(6)	5.4444(8)	8.0186(10)	16.464(4)
<i>c</i> (Å)	8.804(2)	21.173(4)	25.208(3)	37.494(4)	17.972(6)
α (°)	90	90	90	90	90
β (°)	112.164(3)	91.208(14)	104.213(12)	90	90
γ (°)	90	90	90	90	90
<i>V</i> (Å ³)	1405.7(6)	1437.8(4)	1836.3(4)	1718.0(4)	1771.9(8)
Space group	<i>P</i> 2 ₁ / <i>c</i>	<i>P</i> 2 ₁ / <i>c</i>	<i>P</i> 2 ₁ / <i>n</i>	<i>P</i> 2 ₁ 2 ₁ 2 ₁	<i>P</i> 2 ₁ 2 ₁ 2 ₁
<i>Z</i>	4	4	4	4	4
<i>T</i> (K)	293(2)	298(2)	298(2) K	298(2) K	298(2) K
ρ_{calcd} (g cm ⁻³)	1.263 Mg/m ³	1.535	1.509 Mg/m ³	1.524 Mg/m ³	1.647 Mg/m ³
μ (mm ⁻¹)	0.081 mm ⁻¹	2.858	2.260 mm ⁻¹	2.405 mm ⁻¹	2.351 mm ⁻¹
θ range (°)	1.89 – 26.49	3.28 – 25.00	3.04 – 24.99	2.76 – 25.00	2.72 – 28.89

<i>h / k / l</i>	-9,9/-	-12,14 /-6, 6/	-16,9/-6,6/-	-5,6/-9,6/-	-7,6/-20,16/-
indices	26,26/-10,10	-17,25	28,29	34,44	8,24
Reflections collected	14035	5475	6601	4431	5286
Unique reflection, R_{int}	2788 [R(int) = 0.0335]	2536 [R(int) = 0.0489]	3240 [R(int) = 0.0452]	2784 [R(int) = 0.0472]	3734 [R(int) = 0.0408]
GooF	1.044	1.000	0.965	1.064	0.965
$R1[I > 2\sigma(I)]$	0.0445	0.0630	0.0468	0.0566	0.0564
$wR2[\text{all data}]$	0.1157	0.1308	0.1105	0.1082	0.0949
$\Delta\rho_{\text{max}}, \Delta\rho_{\text{min}}$ (e Å ⁻³)	0.160, -0.222	0.364, -0.518	0.352, -0.393	0.290, -0.376	0.465, -0.565

Crystallographic data has been deposited for compounds **4c**, **4k**, **4r**, **4s** and **4t** with the Cambridge Crystallographic Data Centre [CCDC 1037001/2/3/4/5 respectively]. Copies of the data can be obtained free of charge at www.ccdc.cam.ac.uk/conts/retrieving.html.

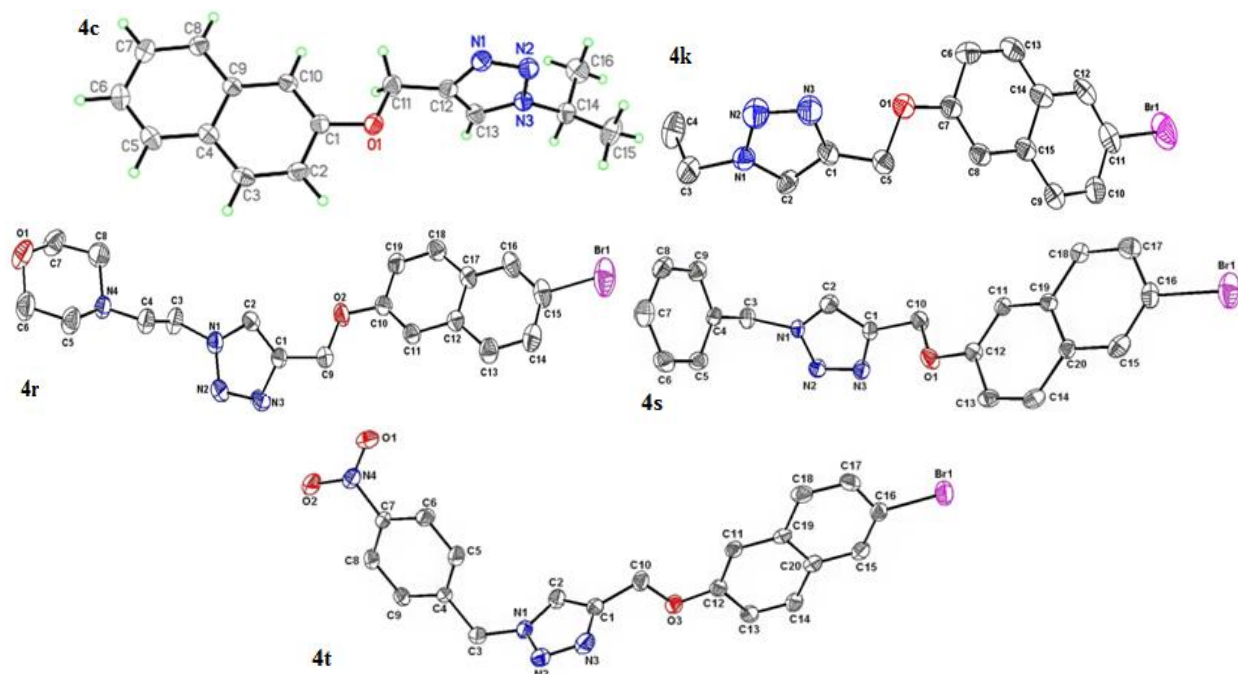


Figure 1: ORTEP drawings (30% probability level) for **4c**, **4k**, **4r**, **4s**, and **4t**

Antiplasmodial activity, DHFR inhibition assay and Cytotoxicity:

Antiplasmodial activity:

P. falciparum 3D7 and Dd2 strains were obtained from the Malaria Research and Reference Reagent Resource Centre (MR4), cell culture reagents and SYBR Green 1 were from Invitrogen, Pyr and DMSO were from Sigma, human serum was from Millipore. Both the strains were grown in RPMI 1640 medium (containing 2 g/litre sodium bicarbonate, 2 g/litre glucose, 25 µg/ml gentamicin, 300 mg/litre glutamine, 10 % human serum, and human erythrocytes at 2% haematocrit) at 37°C in the presence of a gas mixture (5% O₂, 5% CO₂, 90% N₂). Parasites were synchronized by treatment with 5% D-sorbitol at ring stage. Stocks of all the compounds and Pyr were prepared in DMSO at 20-50 mM concentrations, and the stocks were serially diluted 2-fold in 50 µl culture medium across rows of a 96 well tissue culture plate. DMSO (0.05%) or chloroquine (500 nM) was added to the control wells. 50 µl parasite suspension (1% ring-infected erythrocytes at 4% haematocrit) was added to each well. The plate was incubated in a *modular incubator chamber* (Billups-Rothenberg, Inc.) with the gas mixture at 37°C for 50 hours. At the end of incubation, 100 µl lysis buffer (20 mM Tris-Cl, 5 mM EDTA, 0.008%

saponin, 0.08% Triton X-100, pH 7.5) with SYBR Green 1 (at the manufacturer's recommended dilution) was added to each well, the plate was incubated at 37°C for 30 min, and fluorescence was measured (Ex: 485 nm, Em: 530 nm, gain setting: 50) using an Infinite M200 multimode microplate reader (TECAN) as described previously. The fluorescence of chloroquine-treated culture was subtracted from the fluorescence values of cultures treated with compounds/Pyr and DMSO, which adjusted for the background fluorescence. Fluorescence values of cultures treated with compounds or Pyr were normalized as percentage of the fluorescence of DMSO-treated cultures, plotted against concentrations, and analyzed using nonlinear regression analysis to determine IC₅₀ concentrations as described earlier.

DHFR inhibition assay:

P. falciparum was cultured as described above. Trophozoite stage parasites were isolated from a 100 ml culture with 15-16% parasitaemia by saponin lysis, and soluble parasite extract was prepared as has been described earlier. Briefly, the culture was centrifuged at 894g for 5 min, supernatant was aspirated, and the pellet was suspended in 20 ml cold lysis buffer (0.05% saponin in PBS) and incubated in ice for 5 min. The suspension was centrifuged at 12,096g for 5 min at 4°C. The supernatant was discarded, the pellet was suspended in 20 ml lysis buffer, incubated in ice for 5 min, and centrifuged at 12,096g for 5 min at 4°C. The supernatant was discarded, and the pellet was washed three times with cold PBS to remove residual hemoglobin. The final pellet, which contained parasites, was suspended in 10x volume of the DHFR assay buffer (DHFR Assay Kit from Sigma-Aldrich, Product Code CS0340). The parasite suspension was subjected to three cycles of freeze-thaw using liquid N₂. The lysate was sonicated (pulses of 9 sec on/9 sec off) for 3 min at 4°C, centrifuged at 13000g for 15 min at 4°C. The supernatant, which contained cytosolic proteins was transferred to a fresh micro-centrifuge tube, and centrifuged again at 13000g for 30 min at 4°C. The supernatant was called soluble parasite extract and its protein concentration was estimated by Bradford Reagent (Bio-Rad Protein Assay, Catalog #500-0006) using BSA as standard. As DHFR is a cytosolic protein, the soluble parasite extract was assessed for DHFR activity using the DHFR Assay Kit (DHFR Assay Kit from Sigma-Aldrich, Product Code CS0340) according to the manufacturer's instructions. Briefly, reactions were set up in 1 ml assay buffer with 500 µg soluble parasite extract and DMSO (Control, 0.05% final) or inhibitors (50 µM Pyr, 25 µM **4n**, 25 µM **4p** and 25 µM **4t**). The

reactions were incubated for 30 min at room temperature, and centrifuged at 13000g for 1 min to remove any precipitate. The reaction supernatant was supplemented with 60 μM NADPH and 50 μM DHA, and DHFR activity was monitored at room temperature for 30 min at 15 sec intervals as decrease of NADPH absorbance at 340 nm using a UV/Vis spectrophotometer (PerkinElmer). DHFR activity was determined by linear regression analysis as the rate of change in absorbance per min using the Graphpad Prism software and expressed as the percent activity of control reaction.

Cytotoxicity:

Cells were maintained in 60mm dishes, trypsinised when the cells were confluent and seeded at a density of 10,000 cells/well in 96 well plates. The seeded 96 well plates were incubated for 24 hrs at 37 °C incubator with 5% CO₂ and 100% relative humidity. After overnight incubation, cells were treated with compounds **4a-h**, **4j-q**, **4t** and **5b** at different concentrations ranging from 1 μM to 100 μM in triplicates along with control (DMSO) and Doxorubicin as standard inhibitor in the same plate. After 48hr of incubation, the assay was terminated by the addition of 10 μl of 5%MTT and incubated for 1hr at 37 °C. The medium was discarded and the plates were air dried. To these plates 100 μl of DMSO was added per well. Absorbance was measured at 562 nm in a multimode microplate reader (TecanGENios). The sensitivity of the cell lines to the test compound was expressed in terms of IC₅₀, a value defined as the concentration of compound that produced 50% reduction as compared to the control absorbance. IC₅₀ values are indicated as means \pm Standard Deviation of three independent experiments.

Table 3: *In vitro* antiplasmodial activity^a and Cytotoxicity^b of the synthesized compounds

Compound ID	P. falciparum 3D7	P. falciparum Dd2	IC ₅₀ +SEM (μM)
	IC ₅₀ in μM	IC ₅₀ in μM	HEK-293
4a	97.5	–	NC
4b	54.5	–	NC
4c	43.45	–	NC

4d	61.5	–	NC
4e	46.45	–	NC
4f	48.6	–	NC
4g	38.95	–	NC
4h	80	–	NC
4i	NA	–	–
4j	39.65	41.65	NC
4k	23.55	34.16	NC
4l	22.05	36.93	NC
4m*	21.0	24.0	NC
4n*	19.6	31.03	NC
4o	26.25	–	NC
4p	21.25	–	NC
4q	27.3	–	NC
4r	NA	–	–
4s	NA	–	–
4t*	14.7	13.6	NC
4u	NA	–	–
4v	NA	–	–
5a	NA	–	–
5b	41.45	–	NC

Pyr	0.047	33.95	–
Doxorubicin	–	–	3.13 ± 0.01

^a Pyr was used as a control drug. The IC₅₀ values are average with a standard deviation from two independent experiments, each done in duplicates. NA: Not Active (Did not inhibit, even at the highest concentration used), – : not determined. *More potent than Pyr against resistant strain.

^b Cell line was treated with different concentrations 1μM to 100μM of compounds for 48 h. Cell viability was measured employing MTT assay. IC₅₀ values are indicated as the mean +/- SD of three independent experiments. NC: Non Cytotoxic.

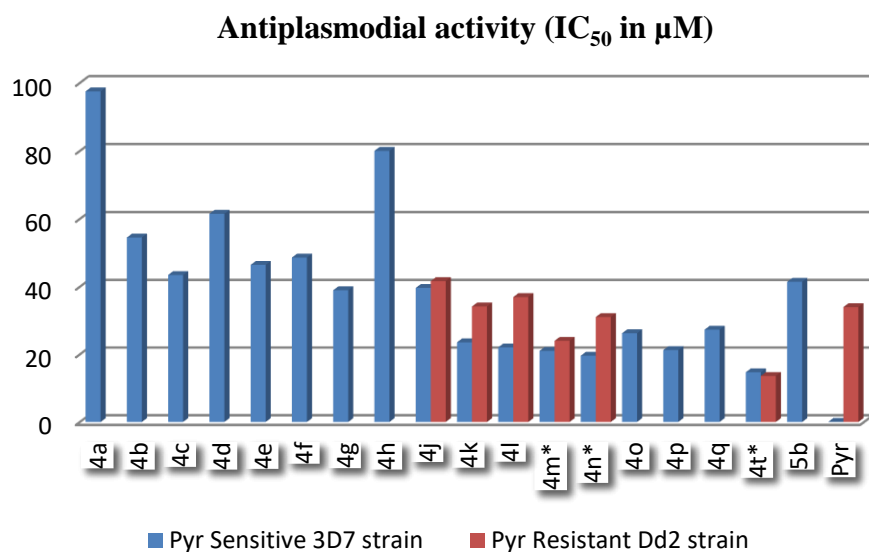


Figure 2: Graphical representation of antiplasmodial activity.

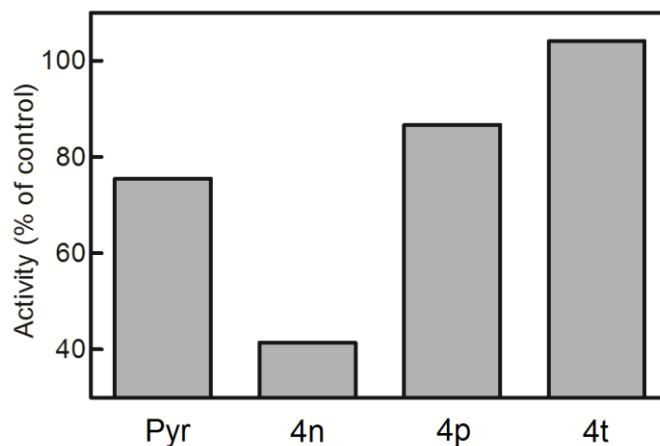


Figure 3: Inhibition of DHFR activity

Docking studies on Pf DHFR:

Docking simulations were performed on active compounds (**4j**, **4k**, **4l**, **4m**, **4n**, **4t**) against DHFR to validate the SAR of triazole derivatives. All these compounds were found to occupy central region in the active site similar to Pyr and an over lay of the dock poses clustered at the same position i.e., naphthol ring is shown in Figure 4. The dock pose of **4t** and Pyr in the crystal structure of PfDHFR (PDB ID: 1J3K) is presented in Figure 5a and 5b. Docking analysis revealed that amino acids Asn108, Phe58, Phe116, Arg59 and Arg122, in the binding pocket of mutant enzyme (1J3K) played a vital role in stabilizing the conformation of **4t**, by π - π staking interactions (Figure 5a). From the ligand interaction diagram (Figure 6a and 6b) it can be clearly seen that the bromo naphthyl group is oriented diametrically opposite to amino acid Asn108 unlike the Pyr, reducing the steric repulsions between bulky side chain of Asn108 and the Br atom of the bromo naphthyl group of triazole derivatives. Additionally, the bromo naphthyl group is projecting into the hydrophobic pocket and exhibits strong π - π interactions with the active site amino acid Phe58. High inhibitory potential of **4t** may be explained on basis of additional π - π interaction between benzene ring of *p*-nitro benzyl group and amino acid Phe116. Dock pose analysis of **4t** also shows polar interactions of $-\text{NO}_2$ with Arg59 and Arg122 of PfDHFR respectively. The computational parameters like IFD score and Emodel (-9.40 & -83.69 respectively) of potent molecule **4t** against mutant PfDHFR 1J3K, surpass that of the existing antimalarial drug Pyr (-9.05 & -69.14 respectively). Against wild type PfDHFR 1J3I, IFD score and Emodel of **4t** (-8.65 & -79.27 respectively) are less compared to Pyr (-10.05 & -84.96 respectively) and this is in good agreement with the antimalarial activity.

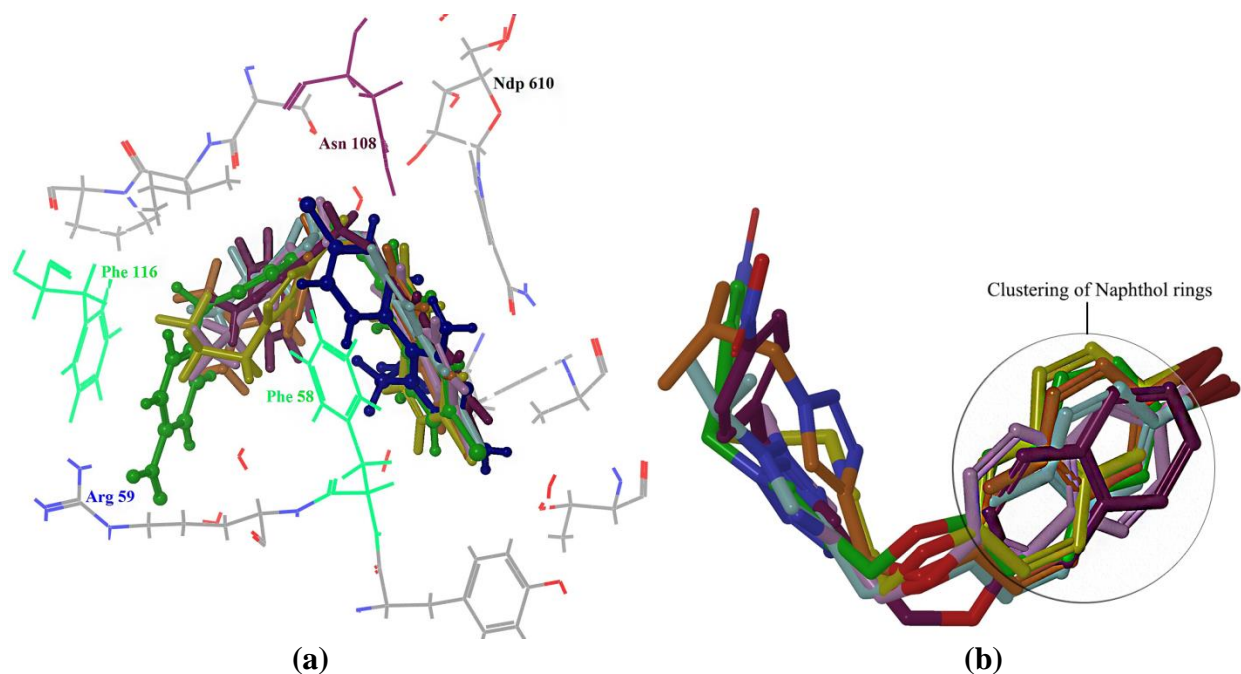


Figure 4: (a) All the docked conformations occupy the same position in the center of the active site with respect to Pyr (blue in color). (b) Overlay of dock poses of **4t** (green), **4n** (orange), **4m** (turquoise), **4l** (yellow), **4k** (plum), and **4j** (maroon).

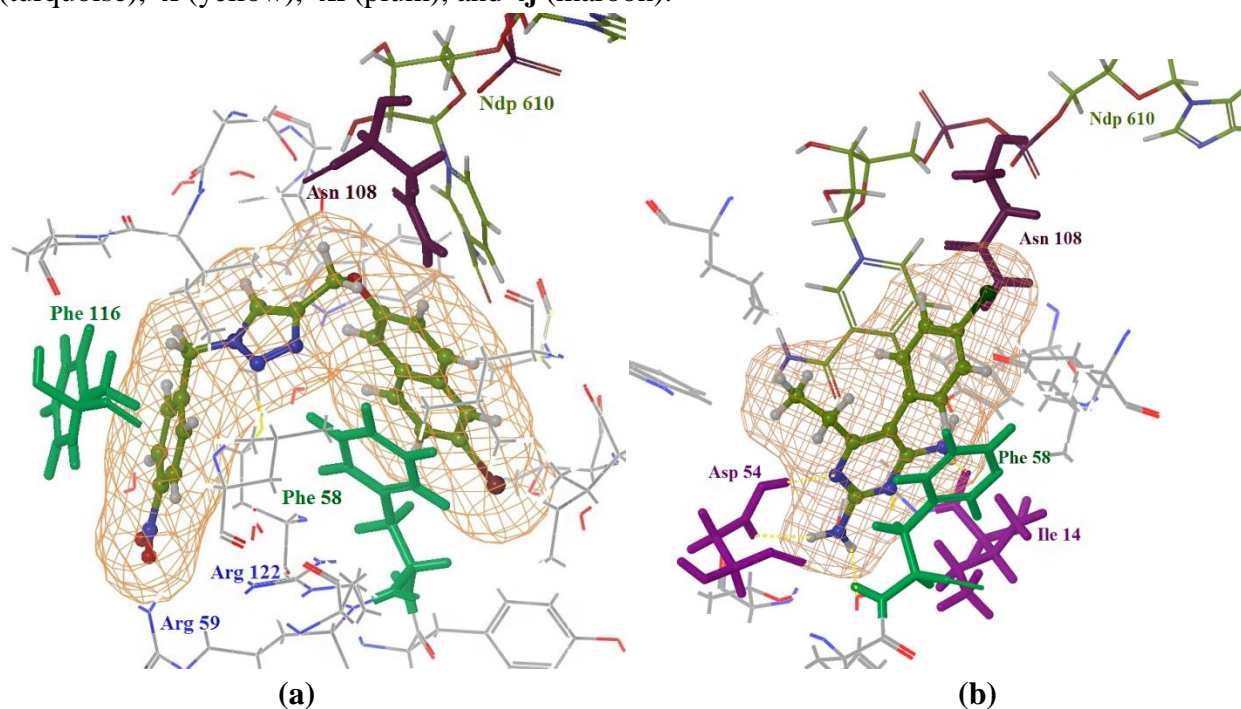


Figure 5. (a) Docked conformation of **4t** in the active site of 1J3K, showing π - π stacking with Phe116 and Phe58, -NO₂ group of **4t** interacting with Arg59 and Arg122. The Br atom on **4t** is away from Asn108. (b) Docked conformation of Pyr in the active site showing π - π stacking with Phe58, four hydrogen bonds with Ile14, Asp54, and H₂O. The Cl atom of Pyr close to Asn108.

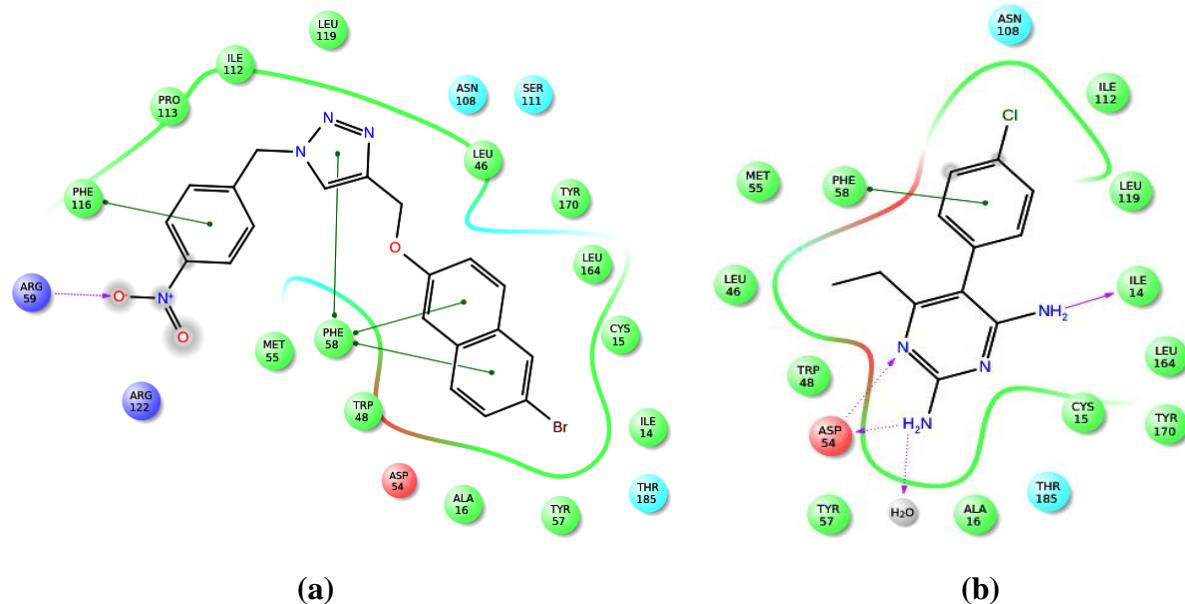


Figure 6. (a) Ligand interaction diagram of compound **4t**, (b) Ligand interaction diagram of Pyr.

The high inhibitory potential of **4t** may be explained on the basis of additional π - π interaction between benzene ring of *p*-nitro benzyl group and amino acid Phe116. Dock pose analysis of **4t** also shows polar interactions of $-\text{NO}_2$ group with Arg59 and Arg122 of PfDHFR. The computational parameters like IFD score and Emodel (-9.40 & -83.69) of a potent molecule **4t** against mutant PfDHFR (1J3K), surpass that of Pyr (-9.05 & -69.14). While in wild type PfDHFR (1J3I), IFD score and Emodel (-8.65 & -79.27) of **4t** are less compared to Pyr (-10.05 & -84.96) and this is in good agreement with the antiplasmodial activity. Dock pose of **4n** in the active site of wild type PfDHFR (1J3I) showed π - π stacking interaction with Phe58 and IFD score and Emodel (-9.12 & -80.24), shown in Fig 7.

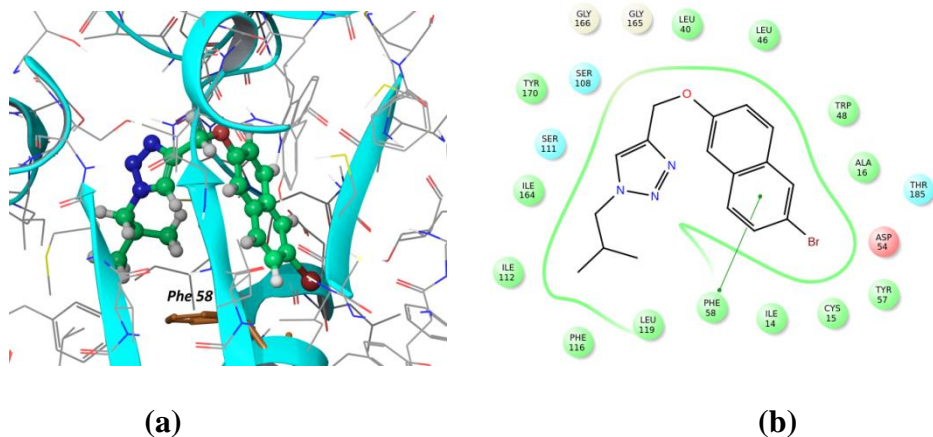


Figure 7: (a) Docked conformation of compound **4n**. (b) Ligand interaction diagram of **4n**.

13. ACHIEVEMENTS FROM THE PROJECT.

- New series of naphthyl bearing 1,2,3-triazoles were synthesized with good yields.
- Novel azide of (*S*)-diethyl-2-(4-azidobenzamido)pentanedioate was synthesized.
- Structures of **4c**, **4k**, **4r**, **4s** and **4t** have been studied by single crystal XRD.
- **4m**, **4n** and **4t** showed potent antiplasmodial activity compared to Pyrimethamine.
- Induced fit docking studies were performed for active compounds.

14. SUMMARY OF THE FINDINGS (IN 500 WORDS)

Novel series of naphthyl bearing 1,2,3-triazoles (**4a-t**) were synthesized and evaluated for their in vitro antiplasmodial activity against pyrimethamine (Pyr)-sensitive and resistant strains of *Plasmodium falciparum*. The synthesized compounds were assessed for their cytotoxicity employing human embryonic kidney cell line (HEK-293), and none of them was found to be toxic. Among them **4j**, **4k**, **4l**, **4m**, **4n**, **4t** exhibited significant antiplasmodial activity in both strains, of which compounds **4m**, **4n** and **4t** (~3.0 fold) displayed superior activity to Pyr against resistant strain. Pyr and selected compounds (**4n**, **4p** and **4t**) that repressed parasite development also inhibited PfDHFR activity of the soluble parasite extract, suggesting that anti-parasitic activity of these compounds is a result of inhibition of the parasite DHFR. In silico studies suggest that activity of these compounds might be enhanced due to π - π stacking. In summary, a new series of naphthyl bearing 1,2,3-triazoles were synthesized by [3+2] cycloaddition of azides with a terminal alkyne in excellent yields. Preparation of triazoles (**4u** and **4v**) bearing *p*-aminoglutamate ester substituent adds another dimension to multifaceted Click chemistry. Most of the synthesized 1,2,3-triazoles exhibited good antiplasmodial activity against wild type strain, among them few compounds are assessed against the resistant strain of *P. falciparum* and exhibited similar potency. Significantly, the compound **4t** was found to be more potent against the resistant strain than the standard antifolate Pyr. The compounds **4n** and **4p** inhibited NADPH depletion activity, suggesting that these compounds target parasite DHFR as the standard antifolate pyrimethamine. The SAR studies of these 1,2,3-triazole derivatives throw light on structural features responsible for antiplasmodial activity. This work will promote further studies in synthesis of naphthyl 1,2,3-triazole derivatives for developing new drugs to combat the widespread drug resistance. All the synthesized compounds are characterized by spectroscopic (¹HNMR, ¹³CNMR, LC-MS and HRMS) data and were found to be in good compliance with their depicted structures. Additionally, the structure of compounds **4c**, **4k**, **4r**, **4s** and **4t** were further confirmed by single crystal X-ray diffraction method. Fig. 2 shows a perspective view of these compounds together with their atomic labeling. Crystallographic data and structure refinement for these compounds is provided in supporting information. Crystallographic data has been deposited for compounds **4c**, **4k**, **4r**, **4s** and **4t** with the Cambridge Crystallographic Data

Centre [CCDC 1037001/2/3/4/5 respectively]. The newly synthesized compounds were evaluated for their antiplasmodial activity against Pyr-sensitive (3D7) and resistant (Dd2) *P. falciparum* strains. Selected 3D7 high active compounds (**4j**, **4k**, **4l**, **4m**, **4n** and **4t**) were assessed for antiplasmodial activity on Dd2 strain. Notably, all these compounds inhibited the growth of Dd2 with similar concentrations to that of wild type strain. The IC₅₀ values of these compounds are summarized in Table 1, and their distribution was configured graphically as shown in Fig. 3. The compounds **4m** (IC₅₀ of 24.0 μM), **4n** (IC₅₀ of 31.03 μM) and **4t** (IC₅₀ of 13.6 μM) against Pyr resistant Dd2 strain showed improved antiplasmodial activity than the control drug Pyr (IC₅₀ of 33.95 μM). It can be concluded that **4m**, **4n** and **4t** showed potent antiplasmodial activity compared to Pyrimethamine.

15. CONTRIBUTION TO THE SOCIETY (GIVE DETAILS)

This was initiated with an aim to combat malarial disease targeting different enzymes that are involved in the development of *Plasmodium falciparum* and to analyze the active site of these enzymes. Based on the architecture of the active site and on already existing antimalarial drugs we have aimed to design new inhibitors that could target the resistance incurred by the parasite. It can be concluded that the newly synthesized molecules have shown better inhibition on resistant type Dd2 strain with improved antiplasmodial activity

16. WHETHER ANY PH.D. ENROLLED/PRODUCED OUT OF THE PROJECT Dr. B. Sai Krishna enrolled for Ph.D and has been awarded Ph,D Degree

17. NO. OF PUBLICATIONS OUT OF THE PROJECT (PLEASE ATTACH)

Synthesis and evaluation of Naphthyl bearing 1,2,3-Triazole analogs as Antiplasmodial agents, Cytotoxicity and Docking Studies

Balabadra Saikrishna^a, Kotni MeenaKumari^a, Manga Vijjulatha^{a,*}, Aparna Devi Allanki^b, Rajesh Prasad^b, Puran Singh Sijwali^b **Bioorganic & Medicinal Chemistry** 25 **2017** 221–232. (Impact factor 2.930)

Molecular docking, 3D-QSAR and Dynamics simulation protocols to explore antimalarial activity of 4-aminoquinoline hybrid derivatives Janaiah Chevula, Saikrishna Balabadra, Sree Kanth Sivan and Vijjulatha Manga* *Journal of Chemical Biology*

(PRINCIPAL INVESTIGATOR)

(REGISTRAR/PRINCIPAL)

(Seal)